

Effect of the Matrix Resin Structure on the Mechanical Properties and Braking Performance of Organic Brake Pads

Hai-Qing Wang,¹ Xing-Yang Wu,² Tong-Sheng Li,³ Xu-Jun Liu,³ Pei-Hong Cong³

¹Key Laboratory for Liquid–Solid Structural Evolution & Processing of Materials of Ministry of Education, Shandong University, Jinan 250001, China

²College of Mechatronics Engineering and Automation, Shanghai University, Shanghai 200072, China

³State Key Laboratory of Molecular Engineering of Polymers, Department of Macromolecular Science, Fudan University, Shanghai 200433, China

Received 16 September 2011; accepted 5 January 2012

DOI 10.1002/app.36751

Published online in Wiley Online Library (wileyonlinelibrary.com).

ABSTRACT: Two chemically modified phenolic resins (PFs) designed and developed for the matrix resins of organic friction materials were characterized. The braking performance of organic brake pads based on the two modified resins and reinforced with hybrid fibers was investigated on a full-scale test bench. The results indicate that the modified PF with more internal friction units possessed much higher impact and compression strengths, greater toughness, and better braking stability. We concluded that the matrix resin with more adjustable struc-

tural units allowed for an adjustable Young's modulus and dynamic mechanical properties and, hence, could indirectly allow an adjustable friction coefficient for organic brake pads during braking process and, furthermore, enable the optimization of braking stability of the friction couples. © 2012 Wiley Periodicals, Inc. *J. Appl. Polym. Sci.* 000: 000–000, 2012

Key words: modification; structure–property relations; viscoelastic properties

INTRODUCTION

Organic brake pads are polymer-based friction materials that generally contain multiple ingredients to achieve a desired performance property, such as a stable friction coefficient, appropriate wear and little damage to the matched brake disc, low noise and vibration, or reliable strength under various braking conditions. The ingredients in organic friction materials mainly include four classes: organic binders, reinforcing fibers, friction modifiers, and fillers. The organic binder is the most important ingredient in friction materials, for it holds all the other ingredients firmly together so that the composites can exhibit the desired performance properties adequately and reliably.^{1–3}

Because phenolic resins (PFs) offer a good combination of thermal, mechanical, and tribological properties and can bind all of the ingredients strongly with little cost, they are generally selected as binders in organic friction materials. However, a normal, straight PF is fragile and rigid. It is easily broken during the braking process; this results in heat fad-

ing, heat expansion, and heat cracks in composite brake pads. The cracks and voids formed are potential safety problems for the braking process, especially under severe operating conditions.^{2,4}

To overcome the shortcomings of a straight PF, various modified PFs have been developed and investigated [e.g., phenol- and alkylether-modified PF,¹ alkyl benzene modified PF, cashew-nut-shell-liquid-modified PF, nitrile–butadiene rubber (NBR) modified PF, linseed-oil-modified PF.^{5,6}] The possibility of four thermosetting resins based on an oxazine ring was also investigated.^{4,7} However, because of the cost factor and problems related to braking performance, these modified resins have not achieved broad industrial application.

It is well known that the polycondensation of conventional PFs catalyzed by hexamethylenetetramine (C₆H₁₂N₄) unavoidably releases volatile products; this results in the formation of microcracks and cavities in the cured products, whereas the polyaddition reaction is free of volatiles. On the basis of this idea, a modified PF was developed as a binder for a hybrid-fiber-reinforced brake pad in our laboratory.⁸ The result proves that the polyaddition curing reaction of the PF resin was effective for improving the integrating properties of the brake pads. This modified resin, called resin A, with a modified PF-carboxylated NBR binary curing structure, has been broadly applied to organic brake pads for railroad passenger coaches in China.

Correspondence to: P.-H. Cong (congph@fudan.edu.cn).

Contract grant sponsor: National Natural Science Foundation of China; contract grant number: 50973021.

Organic brake pads are polymer-based composites with a viscoelastic character. It has been reported that the tribological properties of polymer linings, which are also a kind of organic friction material, are determined by the thermal and dynamical mechanical behaviors of the polymer. An increasing loss factor ($\tan \delta$) or a decreasing storage modulus (E') can provide a polymer lining with greater tribological properties.⁹ That is, increasing the $\tan \delta$ of the matrix binder may be an effective way to develop a brake pad with better integrating properties. A newly modified PF resin with more internal friction units, called resin B, with a PF-epoxy-carboxylated NBR ternary curing structure, was recently designed and synthesized in our laboratory. We hoped that the grafted adjustable structural units in the matrix binder could increase the $\tan \delta$ and friction coefficient because a binder with more adjustable structural units could use internal the friction characteristics to adjust distortion and total friction power, which are related to the friction coefficient and frictional stability.

In this study, the thermal and dynamic mechanical properties of the modified PF resin A, with a binary curing structure, and resin B, with a ternary curing structure, were tested and compared. Organic brake pads for passenger coaches were prepared with resin A or B as a binder. The mechanical properties of the brake pads based on the different binders and reinforced with hybrid fibers were measured against corresponding Chinese standards. The braking performances of the pads were investigated via a full-scale test bench. The objective of this study was to find a way to control the braking performances of organic brake pads.

EXPERIMENTAL

Chemical structure of the modified resins A and B

Figure 1 shows the chemical structure of the modified resins A [Fig. 1(a)] and B [Fig. 1(b)]. The two modified resins had similar chemical structures, with a rigid macromolecular main chain and grafted soft latex particles. The rigid main chains ensured a high mechanical strength and antishearing properties, and the soft latex particles provided a high toughness.

Both resins were rubberlike and very soft. They had the same features:

1. The modification component was a carboxylate rubber, which was generated by the open-ring addition with an epoxy group of the prepolymer generated from a base-catalyzed substitution reaction between straight PF and the epoxy.

2. The soft latex particles were chemically grafted onto the rigid main chains of the macromolecule.
3. The modified resins could form crosslinking structures during the curing process.

The main difference between the two resins was that resin A had a binary curing structure, but resin B had a ternary curing structure. Resin B had more functional units than resin A. Epoxy was selected as the third modification component in resin B because of its very high reactivity; it could cure at lower temperatures and, hence, was easily processed. In addition, the adhesive force of the epoxy was strong enough to ensure suitable mechanical properties in the composites. Moreover, the wear resistance of the epoxy was lower than that of PF. Under a strong friction force, the breaking fragments from the epoxy were PF and butyl carboxyl units, both of which comprise the general binder matrix in friction materials possessing excellent friction properties. Although the original matrix binder of resin B could undergo structural changes under friction and heat activation, the formed fragments could serve the dual functions of adhesion and internal friction; this ensured that the surface films formed after repetitious braking would have relatively stable mechanical properties and stable friction power.

Fabrication and characterization of the brake pads

The material compositions of the brake pads based on resins A and B are shown in Table I. Hybrid fibers composed of carbon fiber, wollastonite whisker, and sepiolite fiber were used as a reinforcer. The contents of all of the ingredients in the brake pads were the same.

The fabrication method for both brake pads was the same. All of the ingredients were completely blended in a Z-type kneading machine to form a molding powder. The molding powder with resin A was hot-pressed at $155 \pm 2^\circ\text{C}$ under 30 MPa for 50 min and was sequentially postcured at $155 \pm 2^\circ\text{C}$ for 50 min. The molding powder with resin B was hot-pressed at $145 \pm 2^\circ\text{C}$ under 30 MPa for 30 min and was sequentially postcured at $145 \pm 2^\circ\text{C}$ for 30 min. The hot-pressed temperatures were obtained from the analysis of the curing temperature for the two resins. The area and thickness of the brake pads were 200 cm^2 and $24_{-0.3}^{+0.2} \text{ mm}$, respectively.

The physical properties (density) and mechanical properties (impact strength, compression strength and modulus, and Rockwell hardness) of the composites were characterized per the corresponding Chinese standards. The test samples were cut from the

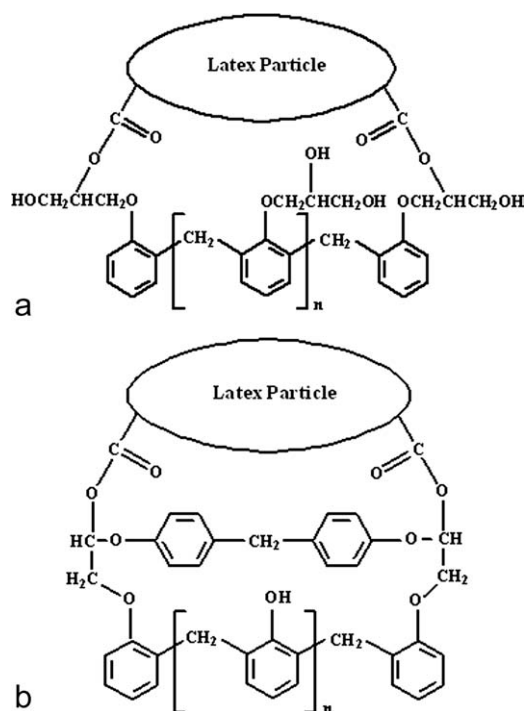


Figure 1 Chemical structure of the modified PFs: (a) resin A and (b) resin B.

pads. Table II lists the measured results of the brake pad testing.

Braking test procedure

The braking tests were conducted on a full-scale test bench. The matched material was a cast steel disc with a diameter of 1250 mm. The pads were placed against opposite sides of the brake disc, and the friction radius on the disc was 448 mm (with a sliding speed of 41.8 m/s at the outer radius of the pad, which corresponded to a speed of 200 km/h). The load on the pads was adjusted to keep the required values; the shaft weight was 10,500 kg. A thermoelectric couple 1 mm under the brake disc surface was used to estimate the nominal temperature of the frictional interface. If the measured temperature exceeded 400°C, the test was stopped automatically.

The braking tests were carried out at room temperature after a 70% conformal contact was established between the matching pad and disc. The applied forces for one test cycle on the pad were 7.5, 5, and 11 kN, and the initial braking speeds were 50, 80, 120, 140, 160, 180, and 200 km/h. Each brake test was done under dry conditions after a cooling interval. The instantaneous friction coefficient was recorded by an attached computer. The average friction coefficient was automatically calculated and given by the computer.

Analysis methods

The curing character of the resins was studied by differential scanning calorimetry (DSC; TGA Pyris 1, PerkinElmer Co., Shelton, USA) at a heating rate of 10°C/min. Thermogravimetric analysis (TGA) was carried out on a thermogravimetric analyzer (PerkinElmer Pyris 1) in a flowing air atmosphere of 40 mL/min and at a heating rate of 20°C/min.

The dynamic mechanical properties of the pure resins were characterized with a dynamic mechanical analyzer (DMA 242, Netzsch Co., Selb/Bavaria, Germany) in compression mode with selected frequencies of 1, 5, 10, 20, and 33.3 Hz. The specimen size was 10 × 3 mm². The temperature ranged from -90 to 185°C and was increased at a rate of 3°C/min.

The morphology of the pad surface after the entire brake test was observed by a digital camera (Sony H-55, Japan) and by scanning electron microscopy (SEM; 5136MM, Tescan SRO, Brno, Czech Republic). The samples for SEM observation were coated with a thin gold film to render conductivity.

RESULTS

Thermal analysis results

Figure 2 gives the DSC curves of the modified PF resins A and B. For resin A, the heat flow showed a broad exothermal peak and a maximum peak around 155°C as a result of the curing reaction. In the case of resin B, a broad exothermal peak was also detected, and the maximum peak was around 146°C. Figure 2 indicates that resin B had a lower curing peak temperature and a broader curing peak width than resin A, so resin B composites should be easier to process than resin A composites during heat molding.

Figure 3 shows the TGA and differential curves (dynamic thermal analysis) for resins A [Fig. 3(a)] and B [Fig. 3(b)] under air flow. The weight loss of resin A mainly appeared in two steps. The first step occurred at about 100–360°C and may have

TABLE I
Material Composition of the Organic Brake Pads Based on Resins A and B

Composition	Mass fraction (%)
Resin A or B	25
Steel wool	16
Hybrid fibers (carbon fiber/wollastonite whisker/sepiolite fiber)	20 (6/10/4)
Flake graphite	3
FeS	2
BaSO ₄	24
CaCO ₃	5
Kaolin	5

TABLE II
Physical and Mechanical Properties of the Organic Brake Pads Based on Resins A and B

Property	Resin A pad	Resin B pad	Test standard
Density (g/cm ³)	2.18	2.13	GB/T 1033-1986
Impact strength (kJ/m ²)	6.1	8.0	GB/T 1043-1993
Compression strength (MPa)	25.4	33.6	GB/T 1041-1992
Compression modulus (MPa)	676	327	
Rockwell hardness (HRR)	83.6	55.5	GB/T 9342-1988

corresponded to a polycondensation reaction. The second weight loss, which started at about 360°C, was caused by resin degradation, and the maximum weight loss rate was 470°C. The weight loss up to 800°C was 78%.

The TGA curve of resin B mainly appeared in three steps [Fig. 3(b)]. The first step was similar to resin A and occurred at 100–360°C, with a weight loss of 8%. The second step of weight loss started at about 360°C. The maximum weight loss rate in this step was at 470°C, but it was accompanied by many small peaks. The weight loss in the second step was 62%. The maximum weight loss rate in the third step was at 517°C. The total weight loss up to 800°C of resin B was 97%.

Obviously, resin B exhibited more complicated weight loss behavior than resin A. This result agreed well with our macromolecular structure design. Resin B contained more functional units, and its epoxy component might have degraded at a low temperature to form other macromolecular structures, which degraded further when the temperature was higher than 500°C.

Dynamic mechanical analysis (DMA)

Both modified resins were typical flexible materials. For a tribological study, it is important to study the viscoelastic characteristics of the flexible materials at various frequencies. According to calculations, the high-speed braking of railroad passenger coaches at 180, 220, and 360 km/h approximately corresponds to frequencies of 16, 20, and 30 Hz, respectively. Thus, DMA measurements of both modified resins at almost equivalent frequencies of 16.6, 20, and 33.3 Hz were conducted. For comparison, DMA measurements at low frequencies of 1 and 5 Hz were also carried out. The variations of E' and $\tan \delta$ of the resins with increasing temperature at different test frequencies are shown in Figure 4.

It is well known that E' represents the elastic behavior, the corresponding temperature of the $\tan \delta$ peak relates to the glass-transition temperature, and the peak height of $\tan \delta$ corresponds to the viscosity of molecular chains: A higher peak implies that the

movement of the macromolecular chains is more difficult. The variation of the E' values of the two modified resins at different frequencies exhibited similar characteristics:

1. The modulus increased with increasing frequency at the same temperature.
2. The modulus decreased rapidly to nearly 0 MPa when the temperature was increased to 80°C for resin A and 50°C for resin B.

After that, the modulus slowly increased with increasing temperature.

It is noteworthy that the modulus of resin B was lower than that of resin A in the same temperature range of –90 to 80°C, but it was higher than that of resin A when the temperature was higher than 150°C. These results indicate that the toughness of resin B was greater than that of resin A when the temperature was lower than 80°C, but the strength of resin B was much higher than that of resin A when the temperature was higher than 150°C. The DSC analysis results (Fig. 2) indicate that the curing temperature for resins A and B was around 150°C. Therefore, it is reasonable to speculate that the crosslink density of the curing macromolecular structure of resin B was higher than that of resin A.

Resins A and B exhibited two $\tan \delta$ peaks at various frequencies. The $\tan \delta$ peaks of resin A were around 15 and 130°C, and those of resin B were about 20 and 145°C. The peaks at the lower temperature were attributed to the energy loss of rubber ingredients, and those at the higher temperature could be attributed to the movement of the macromolecular main chains. The higher temperature for the movement of resin B implied that the crosslink density of resin B was higher than that of resin A. This result agreed well with the designed structure.

The peaks at 15°C for resin A and 20°C for resin B, which represented the energy loss of the rubber

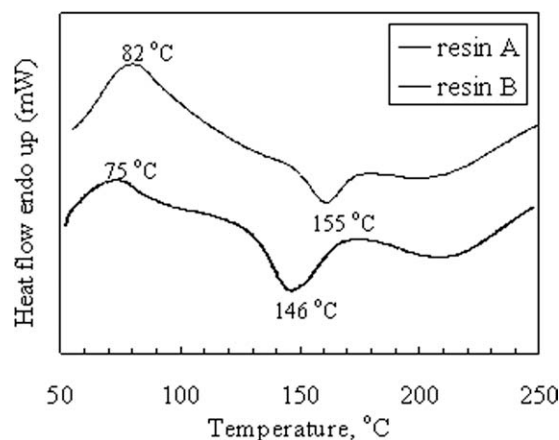


Figure 2 DSC curves of resins A and B.

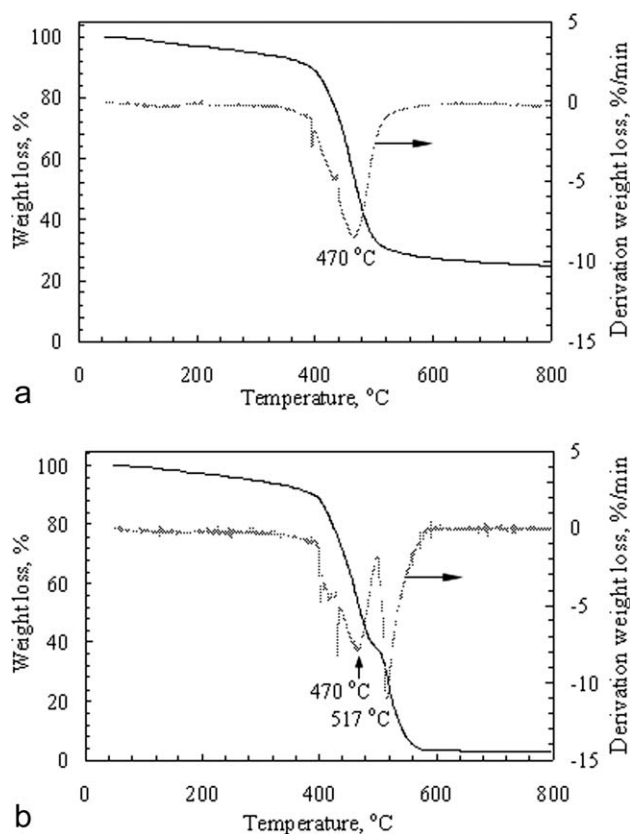


Figure 3 TGA and dynamic thermal analysis curves of the modified PFs under air flow: (a) resin A and (b) resin B.

ingredients, increased obviously with increasing frequency. This result indicates that the rubber ingredient played a more important role in damping at high frequency than the macromolecular main chains. It is well known that $\tan \delta = E''/E'$ (where E'' is the loss modulus); the higher $\tan \delta$ was, the

better was the damping property of the material. Thus, we concluded that the damping property of resin B was better than that of resin A, especially under high-temperature and high-frequency conditions.

The friction power of an organic brake pad comprises adhesive power and distortion power, and the distortion power is mostly dependent on the $\tan \delta$ values of the composites. With an increase in the temperature and frequency, resin B exhibited better damping properties than resin A; this implied that the brake pad based on resin B should have had better friction properties. However, it has been reported^{10–12} that the damping properties of most fiber-reinforced composites are mainly due to the polymer matrix. In this work, hybrid fibers were used as the reinforcer in both brake pads. Fibers with various length-to-diameter ratios may form random reticulations, and the reticulate structure can also supply damping properties.

Physical and mechanical properties of the brake pads

Table II presents the physical and mechanical properties of the brake pads based on resins A and B. All of the test samples were cut from the respective brake pads. It is noteworthy that the impact strength and compression strength of the resin B pad were obviously higher than those of the resin A pad, and the compression modulus and Rockwell hardness of the resin B pad were much lower than those of the resin A pad. These results agreed well with the designed macromolecular structure; resin B, which had a ternary curing structure, indeed exhibited an optimization of the mechanical properties of the brake pad. The more flexible material of the resin B pad, which had a higher impact strength and a

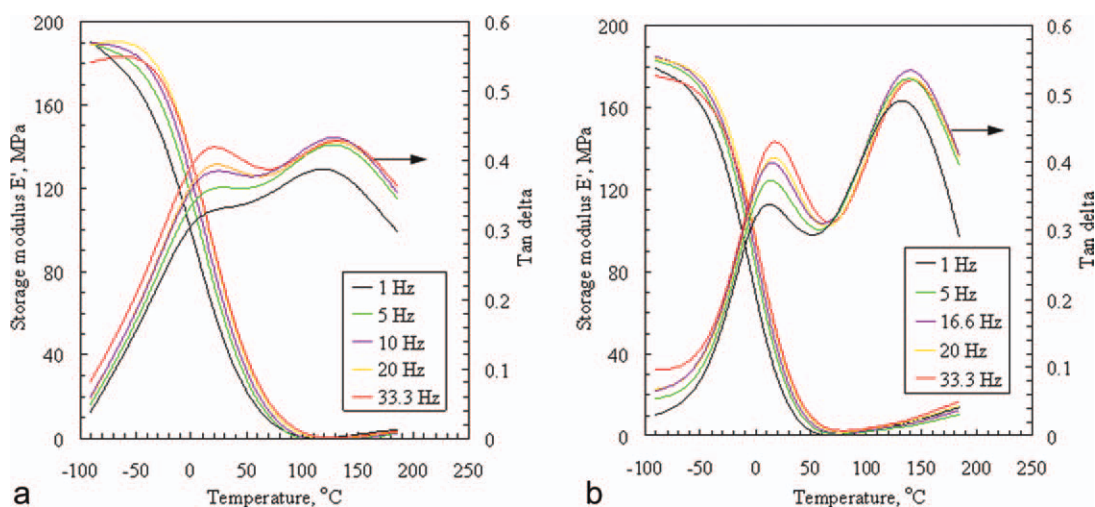


Figure 4 Variation of E' and $\tan \delta$ of the modified PFs with increasing temperature: (a) resin A and (b) resin B. [Color figure can be viewed in the online issue, which is available at wileyonlinelibrary.com.]

TABLE III
Average Friction Coefficients of the Organic Brake Pads Based on Resins A and B Just after Tests where the Brake Pads Had at Least 70% Contact Area with the Brake Disc

Initial speed (km/h)	Average friction coefficient		Temperature (°C)	
	Resin A pad	Resin B pad	Resin A pad	Resin B pad
50	0.291	0.433	53	67
80	0.355	0.420	56	77
120	0.395	0.396	71	84
140	0.396	0.382	72	102
160	0.367	0.372	82	113
180	0.351	0.356	94	125
200	0.337	0.405	103	137

Applied force = 7.5 kN × 2.

lower compression modulus, may effectively prevent the formation of craze during braking and endure more friction heat and high-low temperature shock.

Braking test results

The braking performances of brake pads based on resins A and B were evaluated on a full-scale bench tester. Table III gives the average friction coefficient of the brake pads just after we ran tests in which the brake pads had at least 70% contact area with the brake disc. The applied force on the pad was 7.5 kN. We observed that the average friction coefficient of the resin A pad at various braking speeds ranged from 0.29 to 0.40, and for the resin B pad, it ranged from 0.36 to 0.43. Obviously, the average friction coefficients of the resin B pad at various braking speeds were more stable than those of the resin A pad.

Table IV gives the average friction coefficient of the brake pads during the second cycle of braking tests. The applied force on the pads was also 7.5 kN. The average friction coefficient of the resin A pad at various braking speeds ranged from 0.35 to 0.52, and for the resin B pad, it ranged from 0.29 to 0.38 and was also more stable than that of the resin A pad. The trends for the average friction coefficient during the continuous braking cycle were similar to the results presented in Table IV; this indicated that the resin B pad could achieve more reliable and stable braking than the resin A pad.

Tables III and IV also present the matched disc temperature during the braking tests. The disc temperature increased with the braking speed; the highest temperatures were 137°C for the resin B pad and 103°C for the resin A pad when the braking speed was as high as 200 km/h. It is interesting to note that during the second cycle of the braking test, the disc temperature matched with the resin B pad was

lower than that of the first cycle of the braking test under the same braking conditions. The surface films that formed may have been responsible for this result.

According to Day and Newcomb's model,¹³ which is related to the emergency-stop braking of a train running at 160 km/h, the maximal increase of the average disc surface temperature was 263°C. The temperature increases for the two pads in the tests were much lower than that reported in ref.¹³. It is well known that a temperature increase in the disc should be as low as possible, and this is termed one of the parameters of counterface friendliness. We concluded that both modified resins were friendly to the matched brake disc. This result could have been due to the latex-particle-modified resins themselves having a high flexibility and $\tan \delta$.

Figure 5 shows the wear loss of the brake pads after 36 cycles of braking tests. The wear loss was 0.22 cm³/MJ for the resin A pad and 0.30 cm³/MJ for the resin B pad. Although the wear of the resin B pad was higher than that of the resin A pad, it was suitable wear for an organic brake pad (with the required value for the Chinese standard being <1.0 cm³/MJ). It is well known that an excessively low wear is not good for the brake system because the brake pad should be a self-sacrificing material. An excessively low wear may cause high wear of the matched metallic brake disc, which is much more expensive than the organic brake pad.

Figure 6 shows the micrographs of the worn surface of the resin A and resin B pads after the entire sequence of brake tests. The worn surface of the resin A pad was similar to that of the resin B pad, with some microcracks being observed on both worn surfaces. Discontinuous films were formed, and these adhered firmly to the frictional surface of the resin A pad. The color of the films was somewhat different from that of the pad material.

TABLE IV
Average Friction Coefficients of the Organic Brake Pads Based on Resins A and B During the Second-Cycle Braking Tests

Initial speed (km/h)	Average friction coefficient		Temperature (°C)	
	Resin A pad	Resin B pad	Resin A pad	Resin B pad
50	0.508	0.382	<50	58
80	0.519	0.381	<50	65
120	0.455	0.331	57	79
140	0.426	0.309	76	91
160	0.398	0.302	86	99
180	0.371	0.291	97	111
200	0.352	0.292	108	127

Applied force = 7.5 kN × 2.

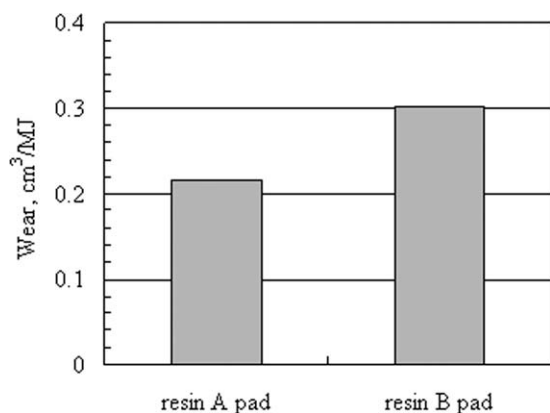


Figure 5 Wear of the organic brake pads based on resins A and B.

In contrast, no obvious films were observed on the frictional surface of the resin B pad. This surface character may have resulted in its higher friction coefficient and wear versus those of the resin A pad.

DISCUSSION

From Table II, we observed that the impact strength of the resin B pad was higher than that of the resin A pad and much higher than the required value of 3 kJ/m² regulated in TB/T 3118-2005. This result indicated that the adhesion between resin B and the other ingredients was quite strong. More important

was that the resin B pad showed a higher toughness and compression strength than the resin A pad. It is well known that a friction material with a greater toughness can better match the brake disc, achieve a higher and more stable adhesive friction power, and hence, may stabilize the braking friction coefficient at high speed to effectively prevent braking impulsion.

Organic friction materials simultaneously possess viscosity and elasticity. Both adhesion and elastic distortion contribute to friction power. At high speed, the adhesion of frictional materials will decrease, and this will be accompanied by the degradation or breakage of the matrix resins so that the adhesion power will decrease with increasing temperature. The DMA measurement results in Figure 4 show that the distortion power of both resins increased with increasing frequency. With increasing frequency (see Fig. 4), the $\tan \delta$ values of both resins increased, but the $\tan \delta$ value of resin B, which had a ternary structure, was higher than that of resin A, which had a binary structure. However, the toughness of resin B was greater than that of resin A. The adhesion power and distortion power of resin B with its high toughness could effectively compensate for each other. Thus, the amplitude of the friction coefficient fluctuated over a small range, and finally, the frictional system achieved stable braking.

It is well known that the surface temperature of brake pads during the braking process can vary from 300 to 900°C.¹⁴ Organic binders in friction

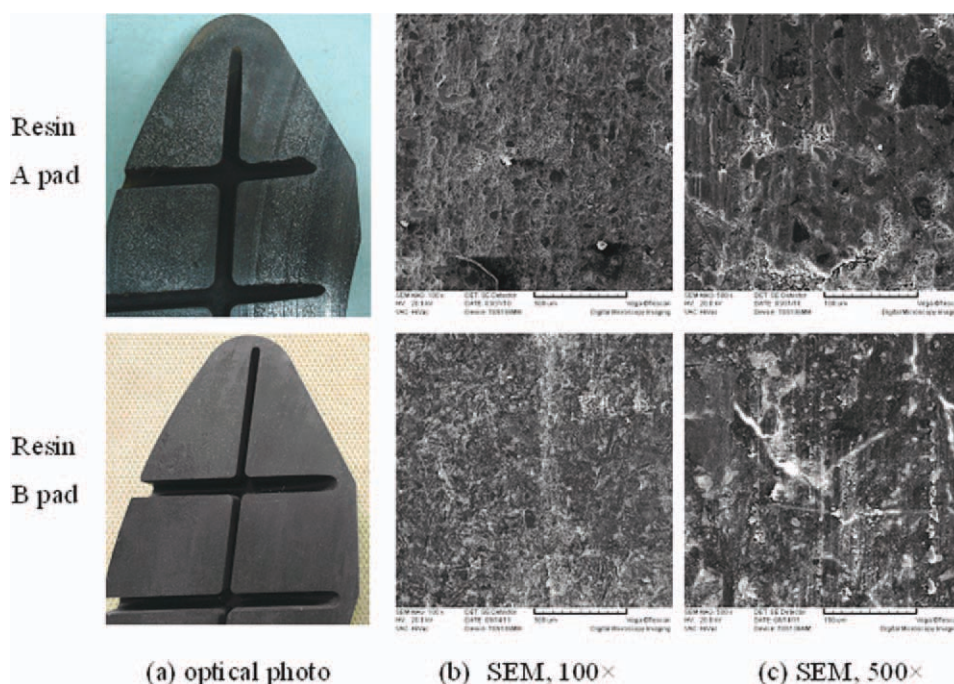


Figure 6 Worn surface micrographs of the organic brake pads based on resins A and B after the whole brake tests. [Color figure can be viewed in the online issue, which is available at wileyonlinelibrary.com.]

materials are most sensitive to the mechanical force and frictional heat, so tribochemical reactions are unavoidable during braking and affect braking performance. These aspects are worth further study, and our results will be reported in the future.

CONCLUSIONS

Two modified PF binders with binary (resin A) and ternary (resin B) macromolecular structures were designed and developed in our laboratory. Brake pads based on the modified PF binders and reinforced with hybrid fibers were prepared, and the braking performances of the pads were investigated on a full-scale test bench.

The resin B pad exhibited a higher impact strength and compression strength, greater toughness, and more stable braking performance than the resin A pad. These results may have been due to the chemical structure of the resin B matrix, which had more functional units than resin A. Resin B exhibited the integrated advantages of its epoxy, PF, and rubber components.

The mechanical properties and toughness of the matrix resin strongly affect the braking performance of an organic brake pad, especially its dynamic mechanical properties. A matrix binder with a high $\tan \delta$ is good for stable braking because it can compen-

sate for decreasing adhesive power during high-speed braking.

We concluded that the adjustment of the macromolecular structure of the organic binder could optimize the mechanical properties of the brake pad and, therefore, enable the braking performance of the brake pad to be adjusted, especially for braking stability. Changing the bonding structure of the rubber-plastic macromolecules and the dynamic mechanical properties may be an effective way to achieve this optimization.

References

1. Kim, S. J.; Jang, H. *Tribol Int* 2000, 33, 477.
2. Kumar, M.; Bijwe, J. *Tribol Int* 2010, 43, 965.
3. Bülent Öztürk, S. Ö. *Tribol Lett* 2011, 42, 339.
4. Gurunath, P. V.; Bijwe, J. *Wear* 2007, 263, 1212.
5. Bijwe, J. *Tribol Lett* 2007, 27, 189.
6. Bijwe, J.; Nidhi, N. M.; Satapathy B. K. *Wear* 2005, 259, 1068.
7. Gurunath, P. V.; Bijwe, J. *Wear* 2009, 267, 789.
8. Wang, H. Q.; Wu, X. Y.; Liu, X. J.; Cong, P. H. *J Macromol Sci Chem* 2011, 48, 261.
9. Peng, Y. X.; Zhu, Z. C.; Chen, G. *Adv Tribol* 2010, 3, 947.
10. Bijwe, J. *Polym Compos* 1997, 18, 378.
11. Chandra, R.; Singh, S. P.; Gupta, K. *Compos Struct* 1999, 46, 41.
12. Finegan, I. C.; Gibson, R. F. *Compos Struct* 1999, 44, 89.
13. Day, A. J.; Newcomb, T. P. *J Automobile Eng* 1984, 198, 201.
14. Kristkova, M.; Filip, P.; Weiss, Z.; Peter, R. *Polym Degrad Stab* 2004, 84, 49.